STATE OF ALASKA

DEPARTMENT OF NATURAL RESOURCES

DIVISION OF GEOLOGICAL AND GEOPHYSICAL SURVEYS

August 1984

Alaska Report of Investigations 84-20

MOISTURE-DENSITY AND TEXTURAL ANALYSES OF MODERN TIDAL-FLAT SEDIMENTS, UPPER KNIK ARM, COOK INLET, ALASKA

By

Randall G. Updike, Nagisa Yamamoto, and Peter W. Glaesman

STATE OF ALASKA
Department of Natural Resources
DIVISION OF GEOLOGICAL & GEOPHYSICAL SURVEYS

According to Alaska Statute 41, the Alaska Division of Geological and Geophysical Surveys is charged with conducting 'geological and geophysical surveys to determine the potential of Alaska lands for production of metals, minerals, fuels, and geothermal resources; the locations and supplies of ground waters and construction materials; the potential geologic and seismic hazards to buildings, roads, bridges, and other installations and structures; and shall conduct other surveys and investigations as will advance knowledge of the geology of Alaska.'

In addition, the Division shall collect, evaluate, and publish data on the underground, surface, and coastal waters of the state. It shall also file data from water-well-drilling logs.

DGGS performs numerous functions, all under the direction of the State Geologist---resource investigations (including mineral, petroleum, and water resources), geologic-hazard and geochemical investigations, and information services.

Administrative functions are performed under the direction of the State Geologist, who maintains his office in Anchorage (ph. 276-2653).

This report is for sale by DGGS for $1. It may be inspected at the following locations: Alaska National Bank of the North Bldg., Geist Rd. and University Ave., Fairbanks; 3601 C St. (10th floor), Anchorage; 400 Willoughby (4th floor), Juneau; and the State Office Bldg., Ketchikan.

Mail orders should be addressed to DGGS, 794 University Avenue (Basement), Fairbanks, AK 99701.

CONTENTS

FIGURES

TABLES

MOISTURE-DENSITY AND TEXTURAL ANALYSES OF MODERN TIDAL-FLAT SEDIMENTS, UPPER KNIK ARM, COOK INLET, ALASKA

By Randall G. Updike[1], Nagisa Yamamoto[2], and Peter W. Glaesman[3]

INTRODUCTION

Substantial growth in both the economy and population has occurred in the upper Cook Inlet region of Alaska during the past 50 yr. This growth extends from Anchorage northward along the east side of Knik Arm to Palmer and Wasilla (fig. 1). Currently, the Alaska Department of Transportation and Public Facilities (DOTPF) is examining the feasibility of a bridge or causeway across Knik Arm. The rapidly expanding infrastructure continues to place greater demands on this region, which includes the tidal flats of Knik and Turnagain Arms. Because these tidal areas may become the site of new port and dock facilities, recreational areas, dredged shipping channels, roads, and bridges, the geotechnical characteristics of the sediments that comprise the flats must be evaluated. These characteristics will dictate future engineering designs of facilities in the tidal-flat areas. This report provides baseline information on the nature of surface sediments exposed on these flats at low tide.

Location of Study Area

Upper Knik Arm is located at the northeastern end of upper Cook Inlet in the Anchorage B-7 NE and B-7 NW (1:25,000-scale) U.S. Geological Survey Quadrangles (fig. 1). The study area is 14 mi (22.5 km) long and varies from 1.5 to 5 mi (2.4 to 8 km) wide, with a total surface area of approximately 41 mi^2 (106 km^2). This segment of Knik Arm is bounded on the south by the communities of Eklutna, Peters Creek, and Eagle River (Municipality of Anchorage) and on the north by the Matanuska-Susitna Borough. The Glenn Highway and Alaska Railroad corridors are located immediately south of the arm and cross the northeastern border of the study area.

Previous Investigations

Several regional marine studies of Cook Inlet have been completed over the past two decades (for example, Kinney and others, 1970; Carlson, 1970; Evans and others, 1972; Gatto, 1976). Detailed geologic studies of sedimentation in Knik Arm have been conducted primarily by Susan Barsch-Winkler and A. Thomas Ovenshine of the U.S. Geological Survey, whose work focused on the physiography, texture, bedforms, and transport-deposition mechanisms at work in the arm (Bartsch-Winkler, 1982; Bartsch-Winkler and Ovenshine, 1984; Bartsch-Winkler and Schmoll, 1984). They have defined the intense, dynamic tidal regime that exists in Knik Arm on a diurnal basis, and have shown that the high-energy environment that results from tides ranging up to 30 ft (10 m)---with velocities of nearly 12 ft/s (4 m/s)---causes dramatic rates of erosion and deposition. In an examination of bedforms exposed in raised tidal flats, Bartsch-Winkler and Schmoll (1984) found what appear to be liquefaction-generated bedding disturbances that may have resulted from seismic events, tidal processes, or freeze-thaw phenomena.

[1]DGGS, Eagle River, Alaska 99577.
[2]Department of Geology, Bates College, Lewiston, Maine 04240.
[3]Department of Engineering, University of Alaska, Fairbanks, Alaska 99701.

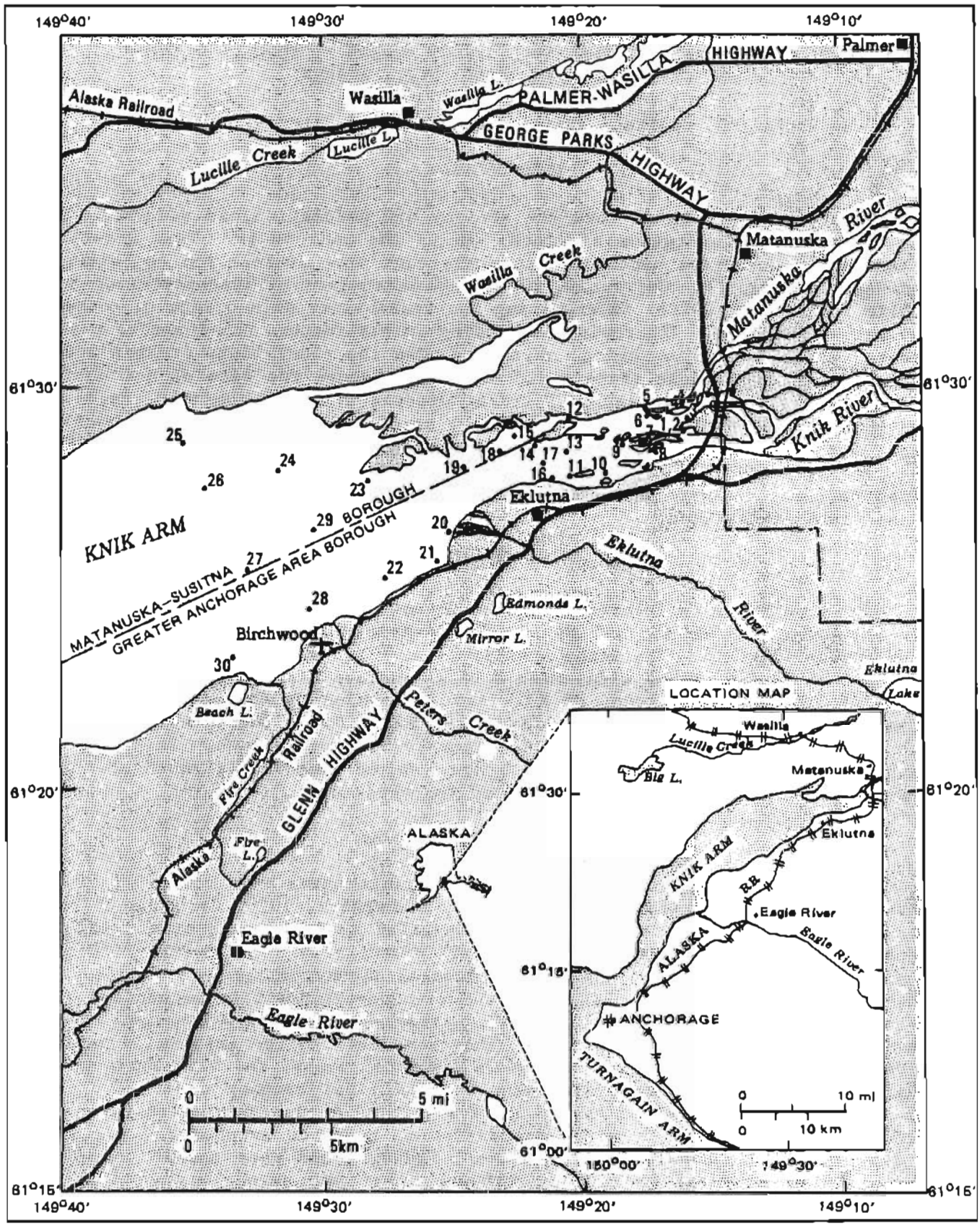

Figure 1. Location of study area, upper Knik Arm, upper Cook Inlet, Alaska. Base from U.S. Geological Survey Anchorage Quadrangle, Alaska, 1972.

Feasibility studies began in 1970 for a Knik Arm bridge crossing (Dames and Moore Consulting Engineers, 1970). Harding-Lawson Associates (1983) is continuing an assessment of the character of subsurface sediments and their suitability to support large engineered structures.

Regional Geology

Knik Arm is an estuary that since Holocene time has been the site of deposition of large amounts of medium- to fine-grained detritus derived from the glacial and fluvial erosion of nearby uplands---primarily the Chugach and Talkeetna Mountains. During the late Pleistocene Epoch, compound valley glaciers advanced into the Knik Arm lowland from the Matanuska and Knik valleys (to the northeast) and terminated just south of the study area. Earlier glacial advances from the uplands that surround Cook Inlet covered most of the lowland with several hundred feet of ice. These glaciations have resulted in the accumulation of hundreds of feet of glacial, glaciofluvial, and glaciomarine sediments in the Knik Arm area.

Although scattered exposures of bedrock occur near the modern shore of the arm (for example, diorite near Eklutna and metavolcanic rocks at the mouth of the Knik River), the lowlands adjacent to the arm are predominantly composed of unconsolidated deposits of Pleistocene age. Knik Arm is an Holocene erosional feature that formed as an extension of the tidal-erosion system of Cook Inlet.

FIELD METHODS

A float-equipped helicopter was used to collect field samples (fig. 2). Sample-site locations were preselected from aerial photographs and confirmed for suitability from the helicopter at an altitude of several hundred feet. Samples were collected as the tide retreated during the morning and early afternoon of May 17, 1983 (fig. 3).

Samples were collected in thin-walled, stainless-steel Soiltest tube samplers that measured 6 in. (15.3 cm) long by 2 in. (5.1 cm) outside diam. The sampler was hand-pushed into the sediment, capped on the exposed end, excavated *in situ*, and capped at the base. Each tube was preweighed and labeled, and the intact sample tubes were packed in a urethane-foam-lined compartment case to minimize disturbance during transport to the laboratory.

LABORATORY PROCEDURES

Laboratory analysis of the sediment cores included determinations of density, moisture content, and particle-size distribution. Upon arrival in the laboratory, the samples were individually weighed in the numbered and preweighed tube samplers to yield the wet mass of each core. The samples were extracted from the tubes with an hydraulic ram ejector. Observational notes were taken on the extruded samples that were then dried for 48 hr in a gravity oven. After the samples were thoroughly dried, they were again weighed to obtain the dry mass. The wet density (γ_s), dry density (γ_d), and natural-moisture content (W_n) of each sample were calculated, and the equations for these calculations are shown in the appendix. Because each

Figure 2. Helicopter on active tidal-flat sediments soon after tide recession. Note surface drainage channels and ripple marks (May 17, 1983).

sample was collected within minutes of emergence from the retreating tide, the cores were obtained under saturated conditions; thus the wet densities are considered equivalent to saturated densities.

Mechanical particle-size analyses used U.S. Standard Testing Sieve nos. 10, 18, 35, 60, 120, and 230 [corresponding to -1, 0, 1, 2, 3, and 4 phi-unit (Ø) sizes, respectively] and a Soiltest CL-392B rotary shaker. Many samples were so fine that over 90 percent of the sample passed the 230-mesh (63μ) screen, and particles occasionally aggregated during shaking on the finer sieves (63 and 125μ). To minimize this problem, the sample was heated 2 to 3 hr immediately before sieving.

Because the samples were predominantly in the silt- and clay-sized fractions, hydrometer particle-size analyses were required following the standard procedure of the American Society for Testing and Materials (ASTM) (1972). A 50-g split of the dry sample was soaked for 12 hr in a mixture of

Figure 3. Tidal-flat surface just prior to sample collections. Note shallow standing water that remains from receding tide (May 17, 1983).

sodium hexametaphosphate and water, which was then agitated in a soil blender for 30 s and washed into a cylinder with sufficient deionized water to bring the volume to 1000 ml. After thorough agitation of the cylinder, hydrometer readings were taken at prespecified time intervals for 24 hr. The first four hydrometer readings (at 30, 60, 90, and 120 s) were taken in triplicate, and the calculated mean values were used for those time intervals.

RESULTS

Particle-size-distribution curves for each core are shown in figures 4-12. ASTM boundaries are used between particle-size classes. From these graphs, it is readily apparent that all samples exhibit similar size distributions, and that consistently fine sand and silt predominate. Textural statistics are shown in table 1.

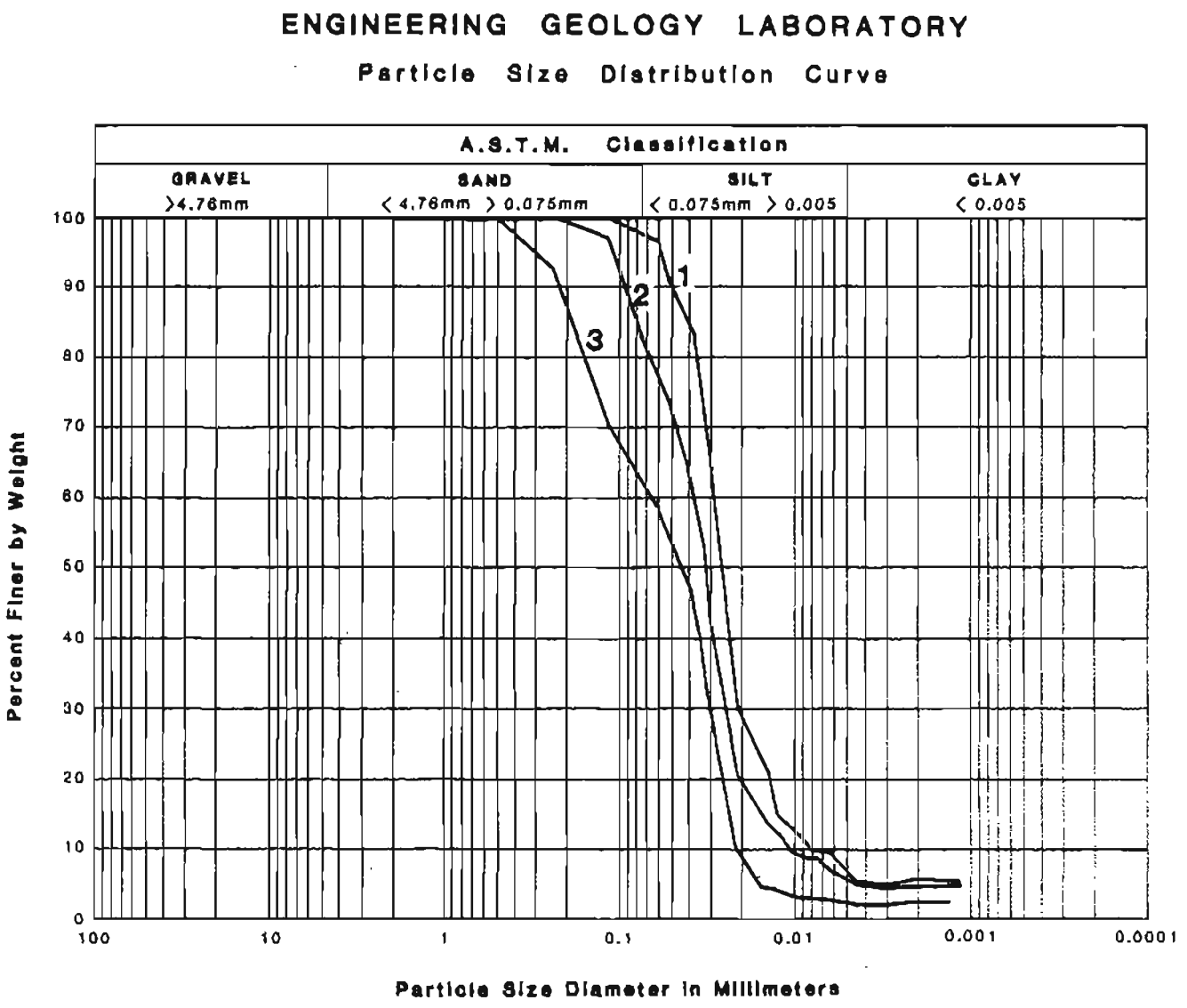

Figure 4. Particle-size-distribution curves, samples 1-3.

The geotechnical properties, including natural-moisture content (W_n), saturated wet density (γ_s), dry density (γ_d), and void ratio (e) are summarized in table 2, which includes field comments. The equations used to calculate physical-property parameters are shown in the appendix.

DISCUSSION

Although all samples fall within a narrow textural range (fig. 13), a distinction may be made between two textural subsets of the population. The distinction is shown by the C-M diagram (fig. 14) introduced by Passega (1964), which plots the coarsest one-percentile (C) in phi notation vs the mean-particle-size class (M) that simultaneously accumulated. The plot shows two domains that indicate the transition from a dominantly tidal-suspension

Table 1. Sedimentary textural statistics (in phi units) for core samples from Knik Arm tidal-flat surface (see fig. 1 for sample-location sites).

Sample no.	Median particle size	Mean particle size	Coarsest one percentile	Sorting	Skewness
1	5.26	5.66	3.40	0.60	0.67
2	4.88	4.85	2.32	1.21	-0.02
3*	4.47	3.85	1.06	1.53	-0.41
4*	4.76	3.89	0.74	1.49	-0.58
5	4.92	4.91	3.06	0.59	-0.02
6	5.06	5.08	3.47	0.57	0.04
7	4.92	5.02	3.18	0.64	0.15
8	4.88	4.81	2.74	0.63	0.11
9	4.92	5.13	3.32	0.75	0.28
10*	4.80	4.78	0.51	0.72	-0.03
11	4.57	4.45	3.06	0.81	-0.15
12	5.44	5.50	4.01	0.66	0.09
13*	2.12	2.08	1.03	0.76	-0.05
14	4.92	4.98	2.94	0.66	0.09
16	4.92	4.78	3.32	0.67	-0.22
17*	2.64	3.11	1.03	1.05	0.45
18	4.72	4.66	3.06	0.72	-0.08
19	4.35	4.40	3.06	0.76	0.07
20	4.54	4.27	2.94	0.80	-0.35
21	4.84	4.93	3.06	0.87	0.10
22	4.76	4.56	2.73	1.50	-0.13
23	5.01	5.19	3.18	0.87	0.21
24	5.50	5.93	2.18	1.45	0.29
25	4.84	4.87	2.94	0.71	0.04
28*	3.56	4.05	1.32	1.49	0.33
29*	4.13	4.19	1.40	0.87	0.07
30*	3.64	3.70	1.32	1.14	0.05

*>30% fine sand.

regime (domain A) to a bottom-current tractive regime (domain B). The suspension domain generally parallels the C=M line (that is, a linear progression of C vs M), while the tractive domain is oblique to the C=M line. This indicates that for domain B the dominant texture varies from medium silt to fine sand, but the coarsest size fraction remains constant. This may reflect either an upper limit of particle sizes available for transport or hydraulic-parameter limits that govern transport (for example, water depth, velocity, or turbulence). Distribution trends of the domains distinguish subtle differences in the depositional regime of the tidal flats; surface morphology was similar at all sample sites.

Samples were consistently collected within several minutes of withdrawal of surface tidal water, and the field party could work safely at a site for less than 3 min before the helicopter landing site began to liquefy. Walking on the surface and vibrations from the helicopter were often sufficient to

Table 2. Geotechnical properties and field notes for surface core samples from Knik Arm.

Sample	W_n	γ_s	γ_d	e	Field comments
1	33.3	1.89	1.42	0.90	Sparse grass; pp=1.6 tsf
2	33.5	1.93	1.44	0.91	No vegetation; pp=0.35 tsf
3	30.8	1.82	1.39	0.83	Sandy, small ripples; pp=0
4	34.9	1.88	1.39	0.94	Sandy, small ripples; pp=0
5	39.5	1.88	1.35	1.07	Ripples = 5 cm amplitude: standing water; sandy
6	41.2	1.84	1.30	1.11	Sandy silt; liquefying ripples; standing water
7	39.6	1.87	1.34	1.07	Sandy; liquefying; ripples
8	33.3	1.90	1.40	0.90	Sandy; liquefying; ripples; midchannel site
9	43.0	1.81	1.26	1.16	Liquefying; ripples; standing water; lateral bar
10	36.8	1.88	1.37	0.99	Side-bar site; ripples
11	34.5	1.92	1.43	0.93	Downstream point; ripples; standing water
12	40.1	1.85	1.32	1.08	Island channel site; small ripples; drained surface
13	32.1	1.94	1.47	0.87	Highly liquefiable sand; main channel
14	39.4	1.85	1.33	1.06	Liquefies quickly; small ripples
15	34.1	1.85	1.34	0.92	Silt surface; tidal crest; planar bedding
16	40.9	1.73	1.23	1.10	Mouth of slough; drained
17	29.6	1.95	1.50	0.80	Main channel; standing water
18	34.6	1.92	1.42	0.93	Lateral channel; just emerged; standing water
19	34.4	1.87	1.39	0.93	Sandy; just drained; small ripples
20	33.3	1.93	1.45	0.90	Offshore cove bar, upstream end; sandy
21	35.9	1.82	1.34	0.97	Liquefying; just drained; small ripples
22	36.0	1.87	1.38	0.97	Main channel; liquefying; small ripples
23	37.3	1.76	1.28	1.01	Silt cover, muddy; well-drained surface
24	36.5	1.84	1.35	0.97	Sandy silt; stable surface
25	53.6	1.70	1.11	1.45	Highly liquefiable
26	34.6	1.84	1.35	0.93	Sandy silt; firmer surface; small ripples
27	38.2	1.83	1.32	1.03	Mid-channel site; standing water; firm surface
28	25.2	1.87	1.50	0.68	Sand; liquefying; large dunes; east of main channel
29	34.2	1.88	1.39	0.92	Sand; liquefying; very hazardous
30	32.2	1.92	1.45	0.87	Silty sand; east side of main channel; ripples

pp = pocket penetration resistance
tsf = tons per ft^2

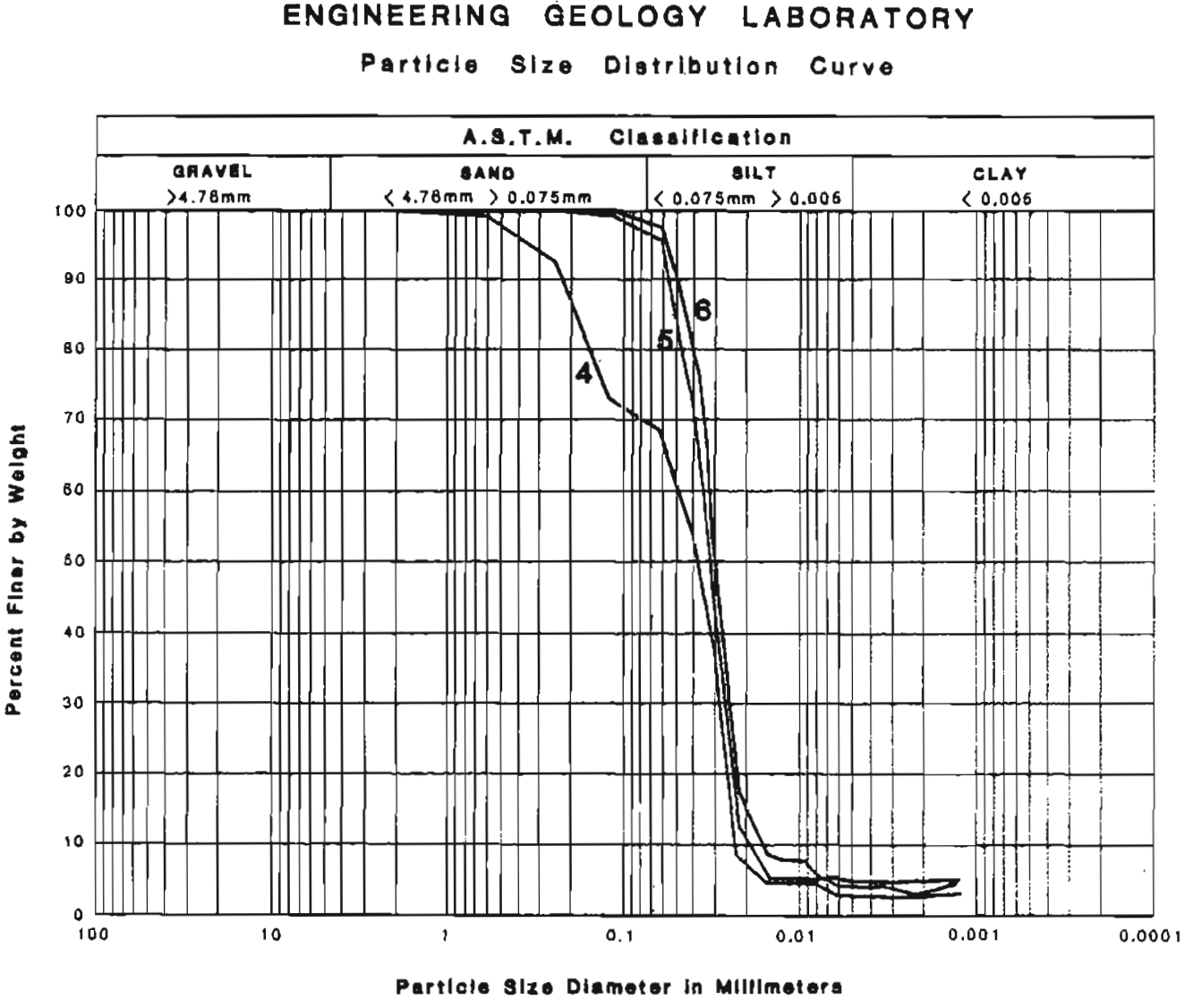

Figure 5. Particle-size-distribution curves, samples 4-6.

generate standing waves in the sandy silt, which suggests that we were sampling sediments in transition from a viscous fluid to a saturated solid. The relationship between water content and solid-particle density should be a continuum from suspension and traction to densified solid. In the suspended state, silt and sand particles are bounded by sufficient water to minimize particle interaction (zero effective overburden pressure). In the low-tide densified state, all particles are in intergranular contact, and maximum effective overburden pressures during the diurnal cycle are reached. At the instant that deposition occurs and surface water recedes, the particles are generally not in contact. The loading effect of a foot or helicopter float is sufficient to develop positive pore-water pressure and induce liquefaction. Without exception, the sites sampled demonstrated this very high liquefaction susceptability after high tide, even though the particles were predominantly silt sized.

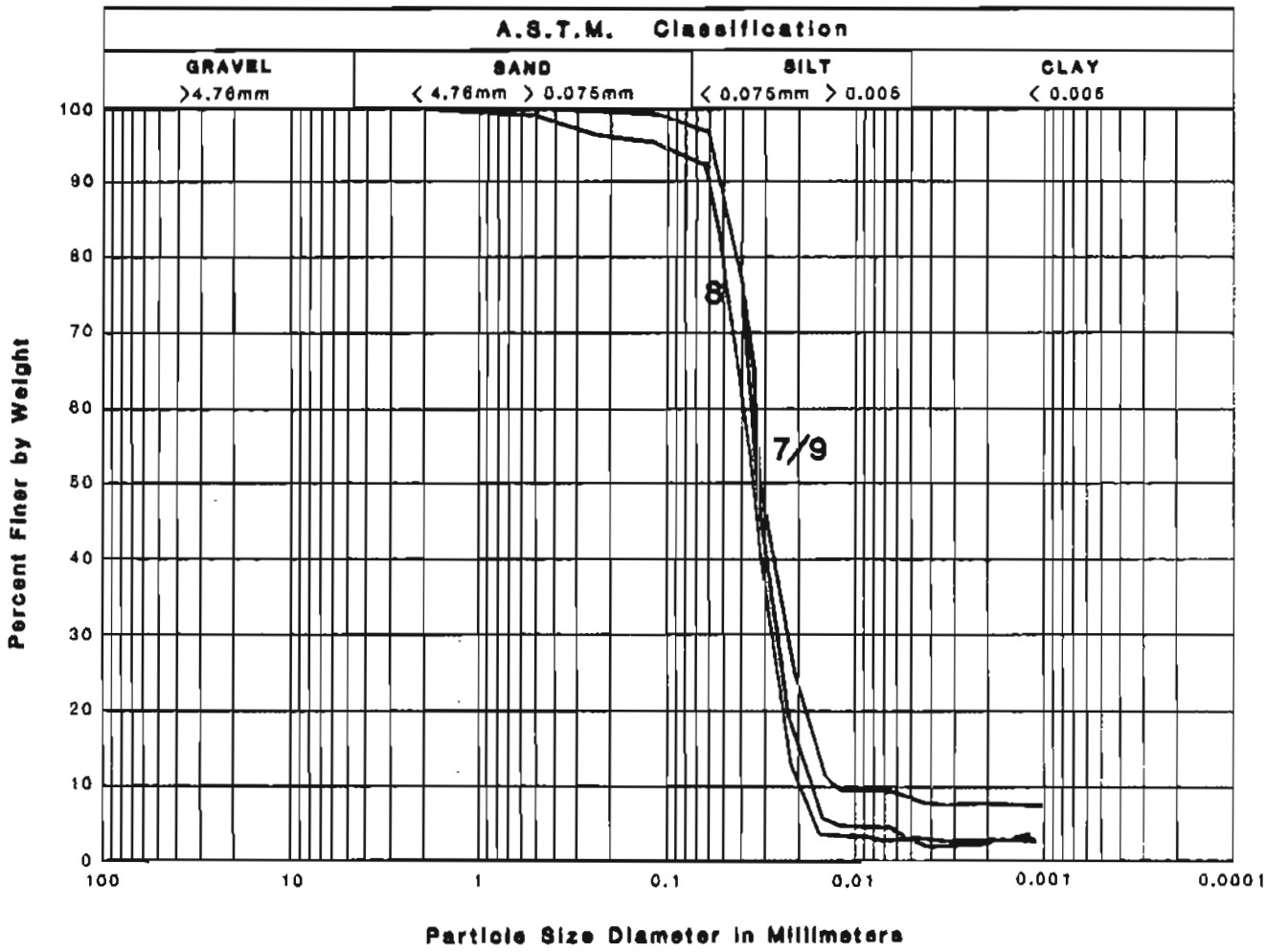

Figure 6. Particle-size-distribution curves, samples 7-9.

The gradational interface from dense suspension to saturated solid is apparent in the plot of sediment dry density (γ_d) vs natural-moisture content (W_n) (fig. 15). Samples representative of the two domains shown figure 14 are distinguished, and the data points form a band across the graph. We believe that the upper boundary (L-line) of this band marks the threshold for quasi-solid-state sediments that have just emerged from the receding tide. Sediments above the L-line behave as a viscous fluid, and those below the line (within the band) as an unstable solid. The lower limit of the band is the limit of saturated conditions (S-line). Below this line, interparticle forces dominate over pore-fluid pressures and liquefaction susceptability diminishes; the two limits are nearly parallel. Equations for these limits are:

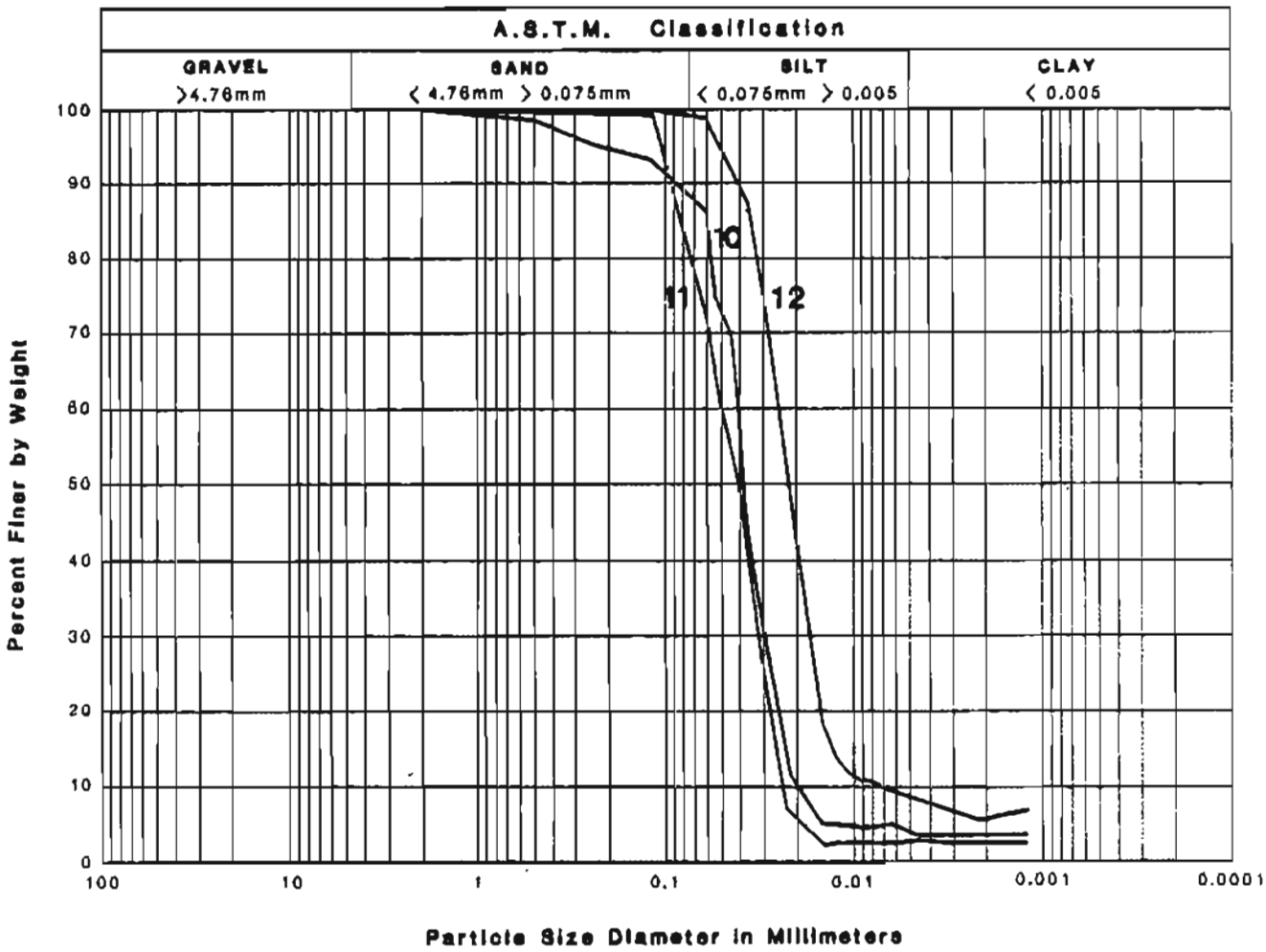

Figure 7. Particle-size-distribution curves, samples 10-12.

L-line: $W_n = -1.4\gamma_d + 54$
S-line: $W_n = -1.4\gamma_d + 48$
where γ_d = dry density (g/cm^3)
W_n = natural-moisture content (%)

If a sample represented by a point on figure 15 is subjected to either shear or normal stresses, it will densify. The point will shift vertically downward due to dewatering, which increases wet density. If draining does not occur when stress is applied, a positive pore-water pressure develops in the sample, and the sample point is displaced across the L-line into the viscous-fluid region, which results in liquefaction. In this instance, W_n increased due to applied stress, and saturated soil density (γ_s) decreased. Conversely, if under the applied stress the soil is allowed to drain, the

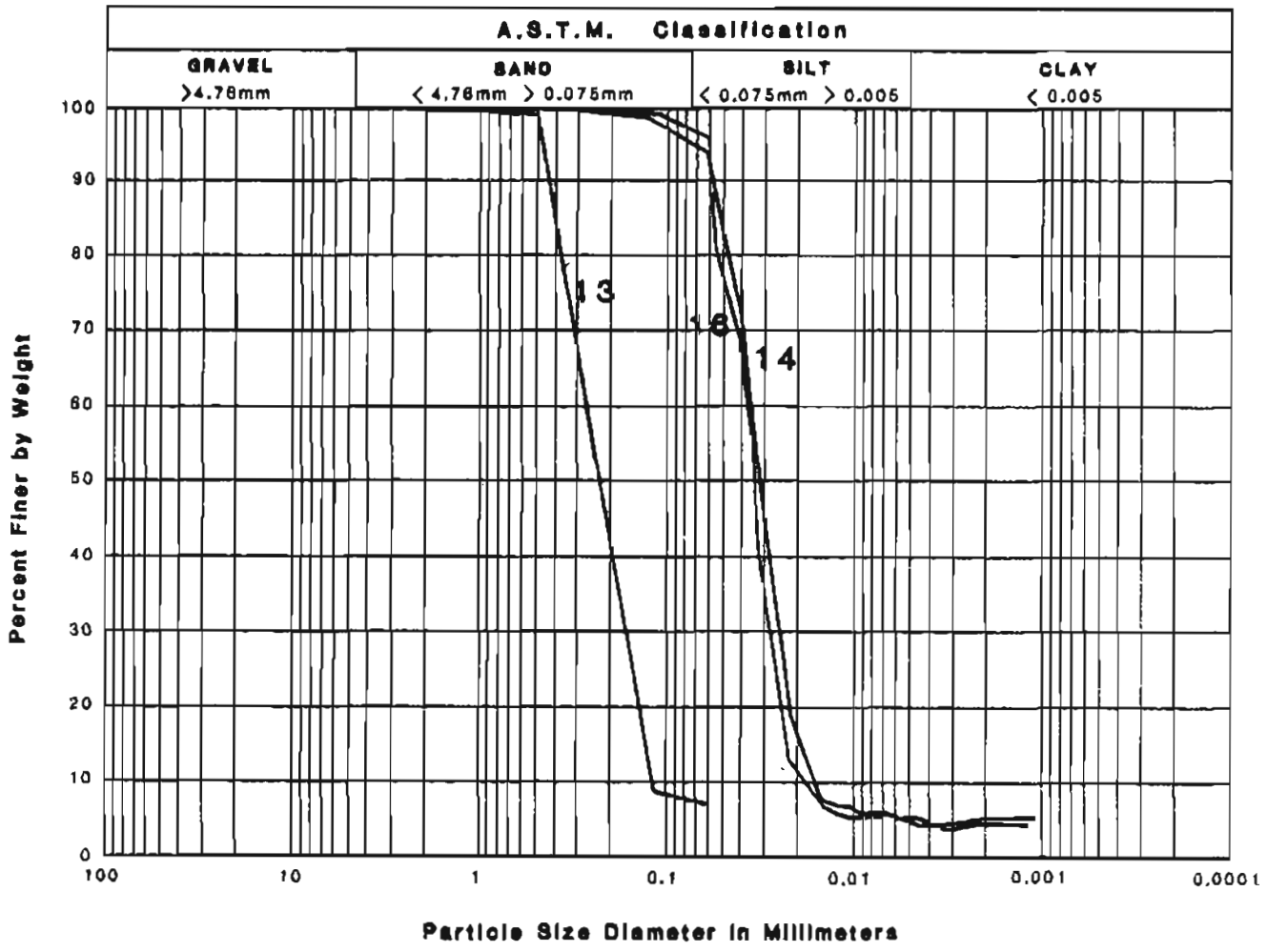

Figure 8. Particle-size-distributuion curves, samples 13-16.

sample point shifts downward to the S-line. If stress continues during drainage, the sample point trends into the densified-sediment region along a path that is dependent on the particle-size distribution, fabric, and rate of drainage of the sediment. Void ratio vs dry density yields a similar plot.

Samples that fell within the sandy domain (B) of figure 14 occur in the lower right corner of figure 15. Because these soils have higher permeability than the finer samples, and because the lower moisture content required an L-line transition, these sediments are more susceptible to liquefaction.

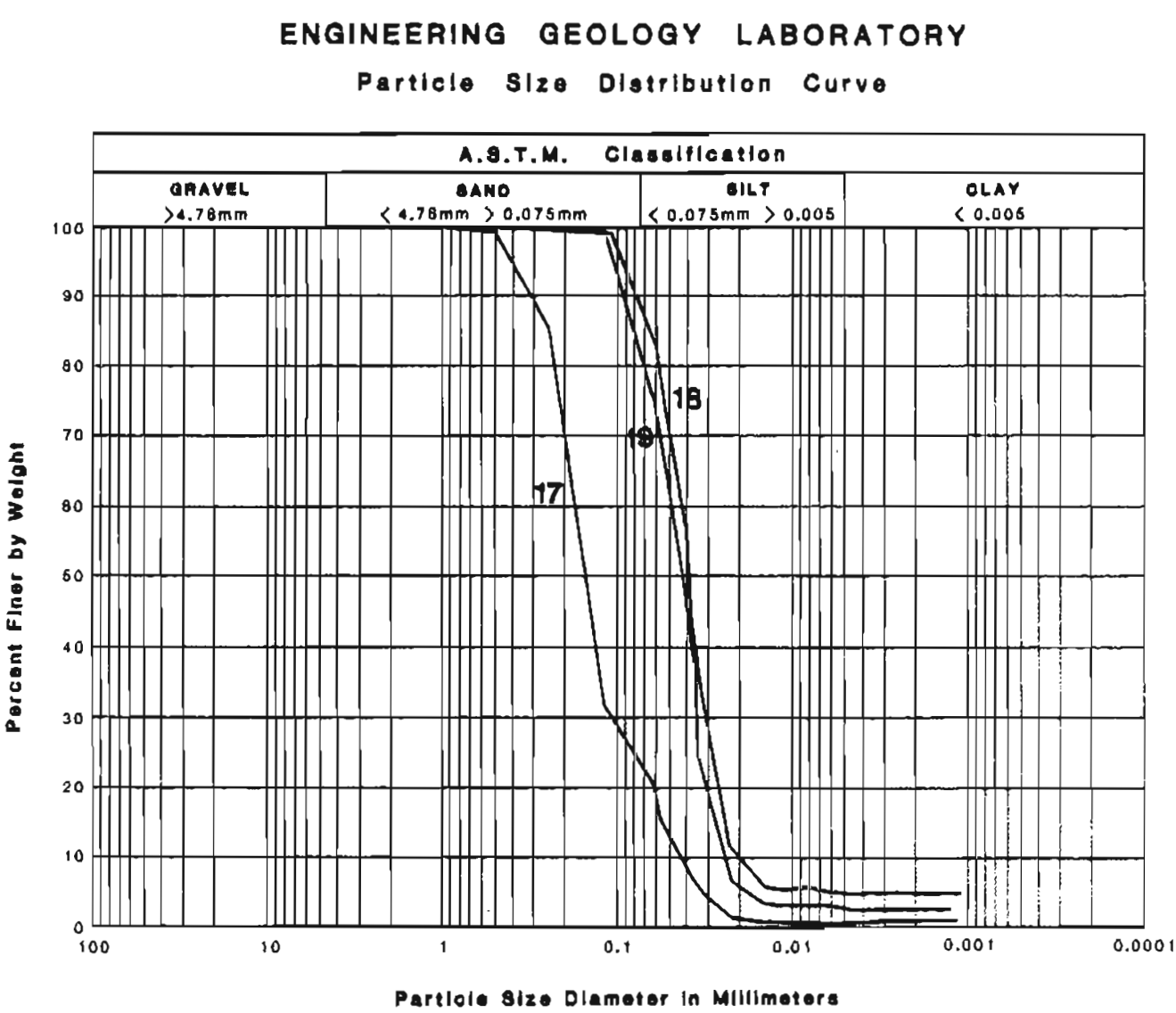

Figure 9. Particle-size-distribution curves, samples 17-19.

We conclude that if traverse or construction activity occurs on the upper Knik Arm tidal flats, the sediments will be susceptable to surface liquefaction. To minimize the surface hazard, the γ_d vs γ_n relationship should fall below the S-line, which may require careful site selection and soil improvement (for example, using vibratory and artificial drainage techniques). If either of these parameters (γ_d or γ_n) can be determined, the limits for that site can be ascertained from the equation in figure 15.

The potential for subsurface, seismically-induced liquefaction to 15 m depth is of concern even though the surface hazard may be reduced, but further geotechnical investigations are necessary to confirm this prediction.

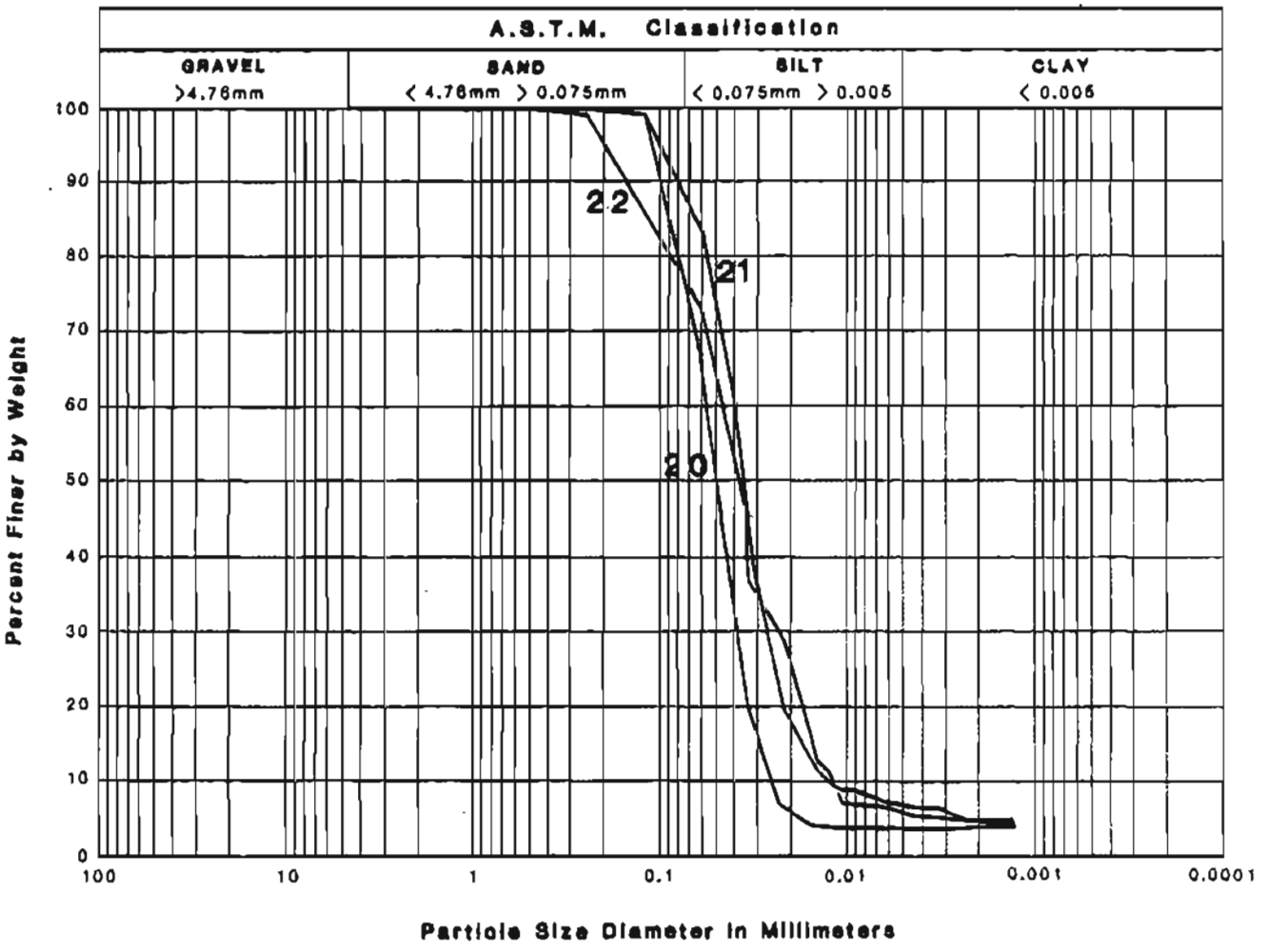

Figure 10. Particle-size-distribution curves, samples 20-22.

REFERENCES CITED

American Society for Testing and Materials, 1972, Standard method for particle-size analysis of soils: American Society for Testing and Materials Specification D-422-63, p. 112-121.

Bartsch-Winkler, Susan, 1982, Physiography, texture, and bedforms in Knik Arm, upper Cook Inlet, Alaska, during June and July 1980: U.S. Geological Survey Open-file Report 82-464, 7 p., scale 1:63,360, 1 sheet.

Bartsch-Winkler, Susan, and Ovenshine, A.T., 1984, Microtidal subarctic environment of Turnagain and Knik Arms - Sedimentology of the intertidal zone: Journal of Sedimentary Petrology [in press].

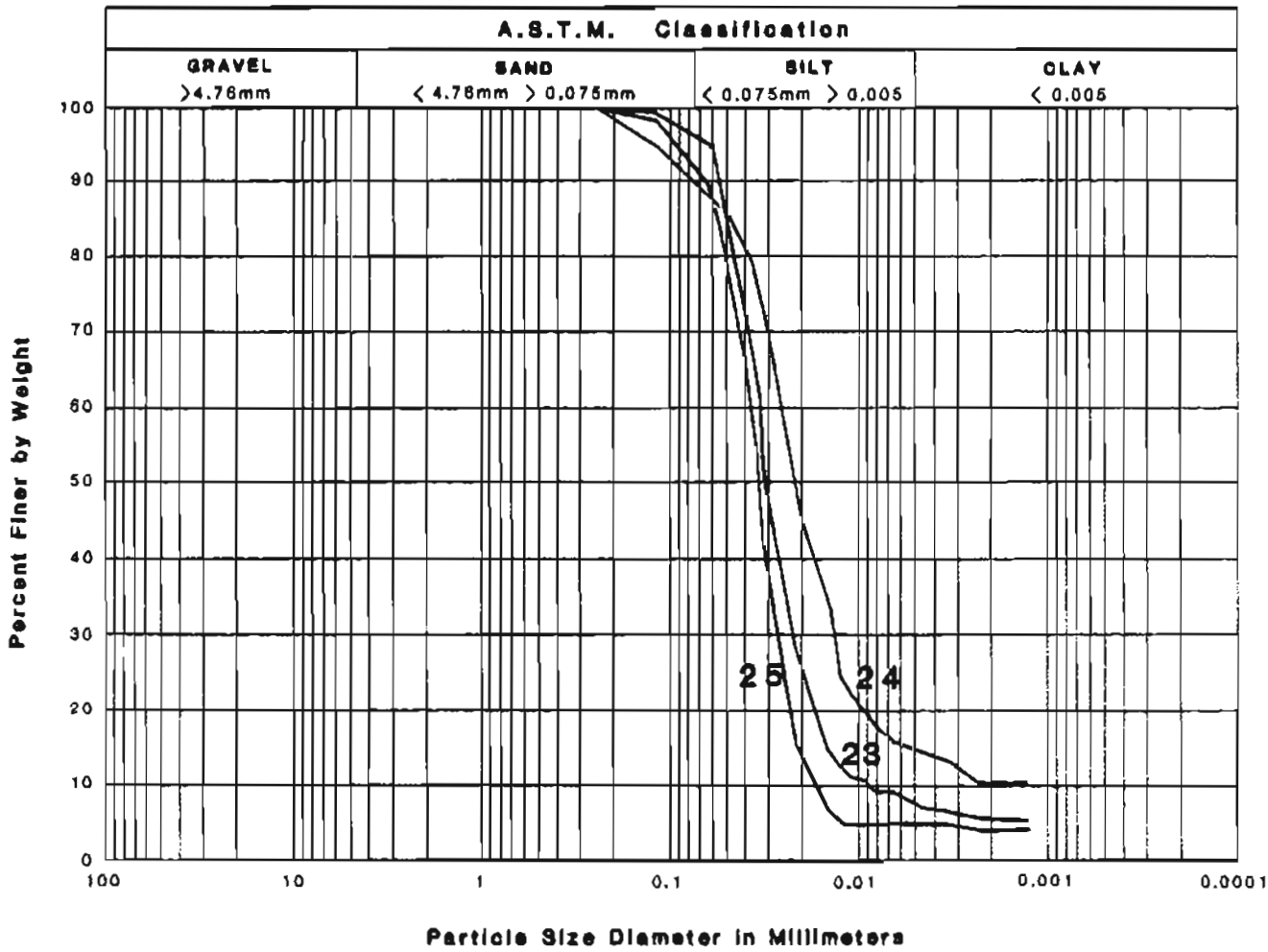

Figure 11. Particle-size-distribution curves, samples 23-25.

Bartsch-Winkler, Susan, and Schmoll, H.R., 1984, Bedding types in late Holocene distributary tidal channel sequences, Knik Arm, upper Cook Inlet, Alaska: Journal of Sedimentary Petrology [in press].

Carlson, R.F., 1970, The nature of tidal hydraulics in Cook Inlet: The Northern Engineer, v. 2, no. 4, p. 4-7.

Dames and Moore Consulting Engineers, 1970, Report of seismic reflection survey, proposed Knik Arm crossing, State of Alaska Department of Transportation: Anchorage, unpublished report prepared for State of Alaska Department of Transportation, 8 p.

Evans, C.D., Buch, E., Buffler, R., Fisk, G., Forbes, R.B., and Parker, W., 1972, The Cook Inlet environment - A background study of available knowledge, Anchorage, Alaska: Fairbanks, University of Alaska Resource and Science Service Center, p. 1-18.

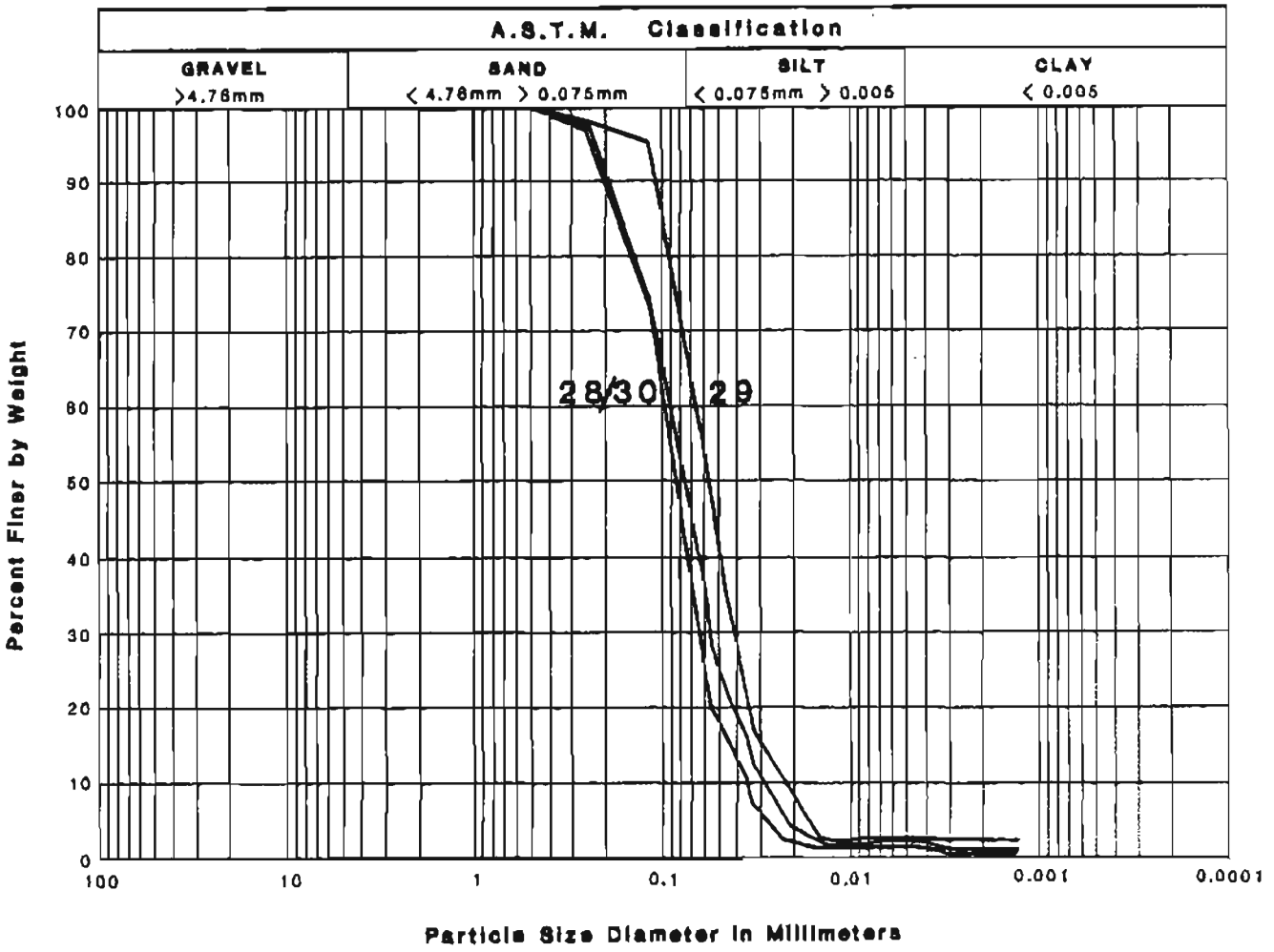

Figure 12. Particle-size-distribution curves, samples 28-30.

Gatto, L.W., 1976, Baseline data on the oceanography of Cook Inlet, Alaska: U.S. Army Corps of Engineers Cold Regions Research and Engineering Laboratory Report 76-25, 81 p.

Harding-Lawson Associates, 1983, Marine seismic reflection survey, Knik Arm crossing, Anchorage, Alaska: Unpublished report prepared for FMPS-Sverdrup, J.V., Consultants, 33 p.

Kinney, P.J., Groves, J.G., and Button, D.K., 1970, Cook Inlet environmental data - R.V. Acona cruise 065, May 21-28, 1968: Fairbanks, University of Alaska Institute of Marine Science Report R-70-2, 120 p.

Passega, R.M., 1964, Grain size representation by CM patterns as a geologic tool: Journal of Sedimentary Petrology, v. 34, no. 10, p. 830-847.

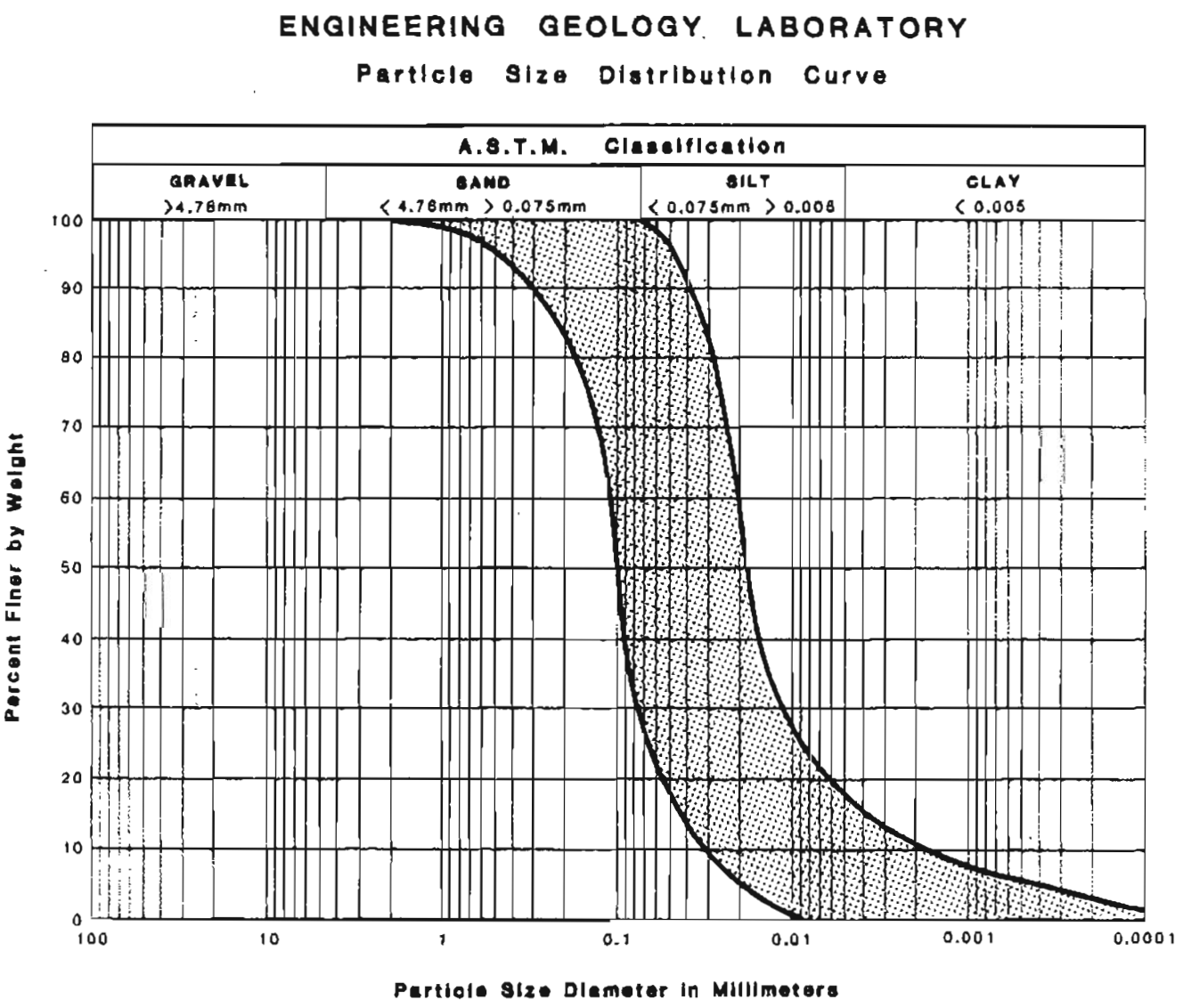

Figure 13. Particle-size-distribution range for all tidal-flat samples, except sand samples 13 and 17.

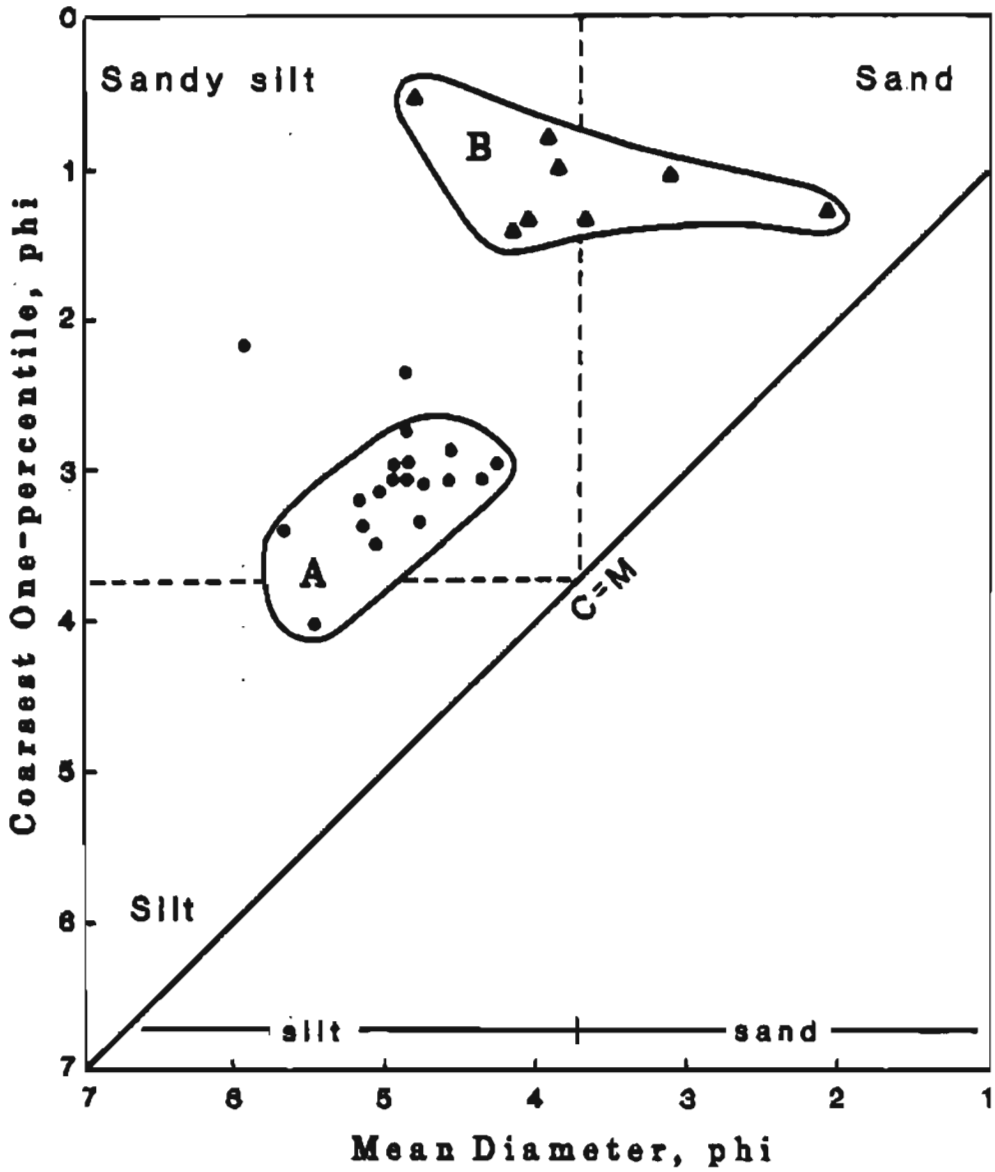

Figure 14. Graph of the coarsest one percentile (C) vs the mean particle size (M) for samples of upper Knik Arm tidal-flat sediments. Diameters are in phi notation. Two domains are distinguished: A (tidal-suspension regime) and B (bottom-current-tractive regime).

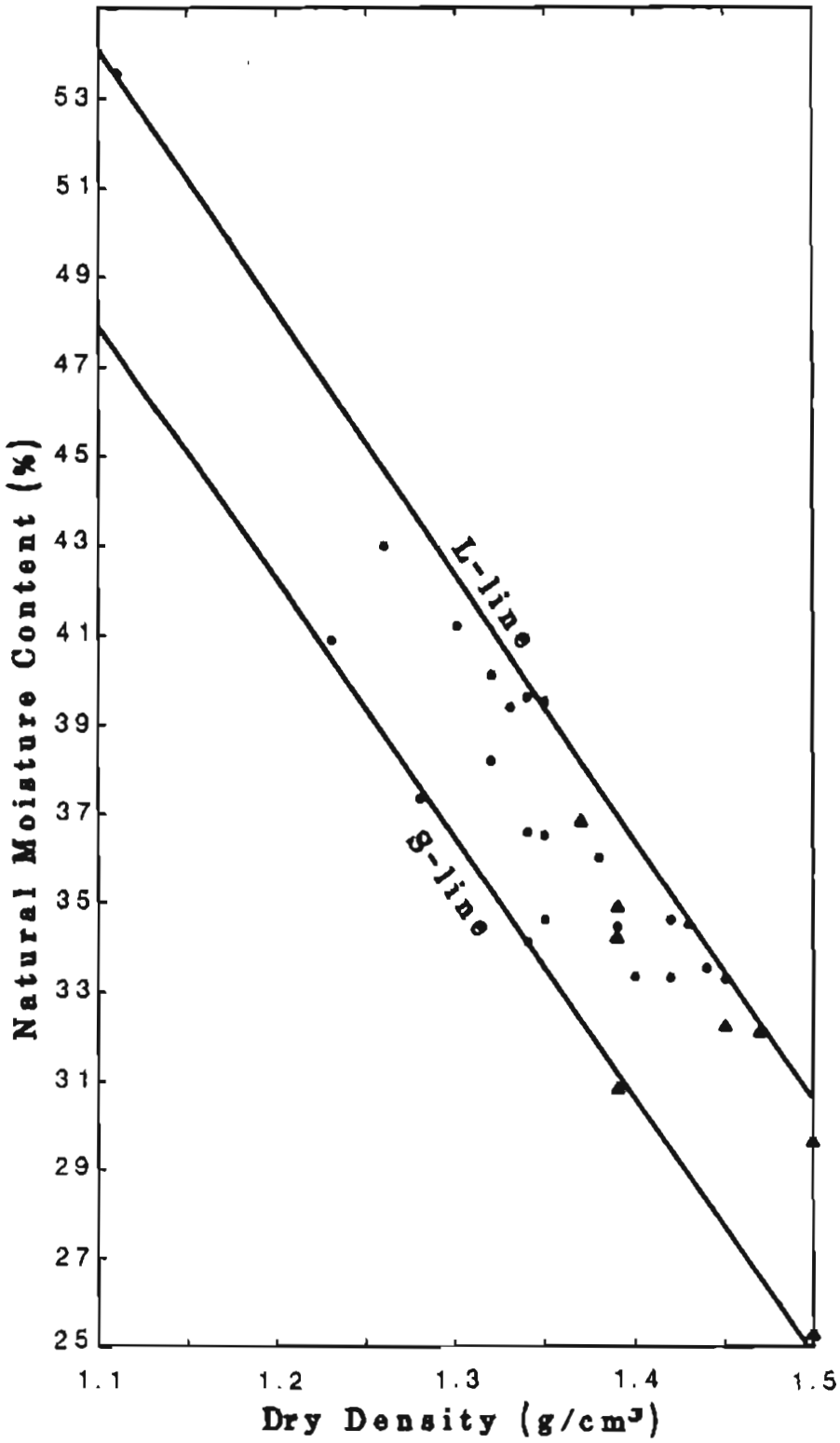

Figure 15. Graph of natural-moisture content (W_n) vs dry density (γ_d) for cores of tidal-flat sediments from upper Knik Arm. Solid circles denote domain A and triangles denote domain B (fig. 14).

APPENDIX
Equations used for calculations

Wet density, $\gamma_s = W_s / V_c$ (g/cc)
Dry density, $\gamma_d = W^w_w / V^c$ (g/cc)
Natural moisture content, $W_p = [100 (W_w - W_p)]/W_p$ (%)
Mean particle size, $M = \frac{1}{2} (\phi_{16} + \phi_{84})$
Sorting coefficient, $\delta_\phi = \frac{1}{2}(\phi_{16} - \phi_{84})$
Skewness, $\alpha_\phi = (M - M_d)/\phi$
Void ratio, $e = V_o/V_s$

Symbols

W_s = mass of solid particles (g)
W^p = mass of saturated soil (g)
V^w = volume of core sampler (cc)
V^c = volume of voids (cc)
V^o = volume of soil particles (cc)
ϕ^s_{16} = particle size at 16th percentile on size-distribution curve (phi units)
ϕ_{84} = particle size at 84th percentile on size-distribution curve (phi units)
M_d = median grain size at 50th percentile on size-distribution curve (phi units)